

Electronic structure of the high- T_c superconductor $\text{Sr}_{0.2}\text{La}_{1.8}\text{CuO}_4$

B. Reihl, T. Riesterer, J. G. Bednorz, and K. A. Müller

IBM Research Division, Zurich Research Laboratory, 8803 Rüschlikon, Switzerland

(Received 26 March, 1987)

Employing ultraviolet and inverse photoemission spectroscopy to study $\text{Sr}_{0.2}\text{La}_{1.8}\text{CuO}_4$, we have obtained a density-of-states type of picture of the electronic structure of this novel material which becomes superconducting below $T_c = 40$ K. Our results compare favorably with recent band-structure calculations.

Possible high- T_c superconductivity has recently been reported for the Ba-La-Cu-O system based on resistivity¹ and susceptibility² measurements. The crystallographic phase in which the probable superconductivity occurs was identified as $\text{La}_2\text{CuO}_{4-y}\cdot\text{Ba}$, which has the K_2NiF_4 structure.² Subsequently, researchers from all around the world have further investigated these and related oxide structures.³⁻⁸ Uchida, Takagi, Kitazawa, and Tanaka³ and Chu *et al.*⁴ confirmed the high- T_c superconductivity (onset temperature above 40 K) for the Ba-La-Cu-O system, while Cava, van Dover, Batlogg, and Rietman⁵ reported a superconducting transition at 36 K for $\text{La}_{1.8}\text{Sr}_{0.2}\text{CuO}_4$. Very recently Wu and co-workers reported superconductivity at 93 K in a mixed-phase Y-Ba-Cu-O compound system which showed only slight pressure effects for the transition temperature.^{6,7}

The mechanisms which are responsible for the superconductivity and, in particular, for the high transition temperatures are unclear at the moment. The search for high- T_c superconductivity in these oxides was motivated¹ by their metallic conductivity together with a possible enhanced electron-phonon coupling because of the formation of Jahn-Teller-type polarons which could be facilitated by the presence of mixed-valent Cu^{3+} and Cu^{2+} ions. Recently, Mattheiss⁹ has performed electronic band-structure calculations for tetragonal La_2CuO_4 which show that the Fermi-surface electrons have substantial O $2p$ character and, in addition, form strong σ bonds with neighboring Cu atoms. Breathing-type oxygen vibrations could then couple very strongly to the conduction electrons at E_F , and hence substantially increase the electron-phonon coupling. The analogous mechanism was used before to explain the superconducting properties of the $\text{BaPb}_{1-x}\text{Bi}_x\text{O}_3$ alloy series.¹⁰ Weber¹¹ has used the energy bands of Mattheiss⁹ to calculate the phonon dispersion and linewidth as well as the electron-phonon interaction. A very strong coupling of oxygen-specific phonons to conduction electrons is found which leads to $T_c \sim 30-40$ K for $\text{La}_{2-x}(\text{Ba},\text{Sr})_x\text{CuO}_4$.

In the present Rapid Communication we have investigated the electronic structure of $\text{Sr}_{0.2}\text{La}_{1.8}\text{CuO}_4$ with ultraviolet photoemission spectroscopy (UPS) at photon energies $h\nu = 21.2$ and 40.8 eV as well as with inverse photoemission spectroscopy (IPS) at an isochromat energy of $h\nu = 9.5$ eV. The density of states (DOS) obtained in this manner is then compared to the calculated total DOS of

Mattheiss.⁹ The overall agreement is quite good. It is interesting to compare the experimentally observed Fermi level with the calculated one, since its energetic position may affect the superconducting properties.⁹

The experiments were performed in a custom-built spectrometer which is housed in a two-chamber ultrahigh vacuum system with a fast interlock for sample introduction. More details of the spectrometer are described elsewhere.¹² The $\text{Sr}_{0.2}\text{La}_{1.8}\text{CuO}_4$ sample was fabricated by solid-state reaction at 1100°C starting from SrCO_3 and the oxides of La and Cu in their appropriate ratios. The product was isostatically pressed into pellets at 1000 bars and 900°C . From the sintered pellets rectangular bars of $2 \times 2 \times 10$ mm³ size were cut, rinsed in methanol, and introduced into the vacuum system by the fast interlock. An anvil-knife-type mechanism was used to fracture the sample *in situ*. The cleanliness and stoichiometry of the surface was checked by Auger-electron spectroscopy (AES). Fresh cleavages exhibited the following AES signal ratios relative to O(503 eV): La(78 eV)=0.82, La(625 eV)=0.12, Cu(60 eV)=0.1, and Cu(920 eV)=0.1. As contaminants we observed only carbon with a signal ratio of C(272 eV)=0.1, which is probably due to using SrCO_3 as a starting material. Altogether five cleavages from two different bars were used. Resistivity measurements⁸ of samples from the same pellet gave superconducting transition temperatures of 40 K.

In Fig. 1 we show combined UPS and IPS data for $\text{Sr}_{0.2}\text{La}_{1.8}\text{CuO}_4$ taken at $h\nu = 40.8$ and 9.5 eV, respectively. As a first result, we note that both spectra show a weak but substantial emission intensity at the Fermi level $E_F = 0$, as is expected from this metallic compound with a measured resistivity of $0.02 \Omega \text{ cm}$ at room temperature.⁸ The spectral intensities right at E_F , which for both spectroscopies was determined from a Ta foil, are used to scale the two spectra in a rough manner (see the $\times 10$ inset in Fig. 1). The different slopes of the emission onsets reflect the slightly different energy resolution (0.2 eV for UPS and 0.35 eV for IPS, Ref. 12).

Besides the metallic emission around E_F we note strong spectral features in the occupied part around -4 eV (denoted *A* and *B* in Fig. 1) and less pronounced structures at -9 eV (*C*) and -16 eV (*D*). Features *E* and *F* in the unoccupied part are much broader. The whole spectrum (occupied and unoccupied) resembles very much that of a semiconductor or insulator with valence (*A, B*)

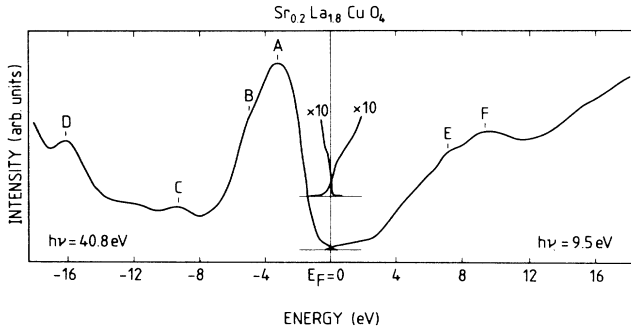


FIG. 1. Ultraviolet photoemission spectra taken at $h\nu=40.8$ eV and inverse photoemission spectra at $h\nu=9.5$ eV from $\text{Sr}_{0.2}\text{La}_{1.8}\text{CuO}_4$. The two spectra are roughly normalized to the spectral intensity at the Fermi-level onsets (see $\times 10$ inset). Features A – F are discussed in the text.

and conduction (E, F) bands. The edges can be determined by drawing tangents to the A and E slopes approaching E_F in Fig. 1. We arrive at -1 eV for the valence-band (VB) edge and $+2$ eV for the conduction-band (CB) edge using the intersects of the tangents with the zero line. This results in a total gap of 3 eV, which should be observable by optical absorption measurements. Indeed, with the exception of the metallic emission the measured electronic structure as presented in Fig. 1 resembles closely that of SrTiO_3 (Ref. 13), which has a perovskite structure. Also the K_2NiF_4 structure, which is the underlying structure of the present $\text{Sr}_{0.2}\text{La}_{1.8}\text{CuO}_4$ sample, can be visualized as single layers of perovskite-type unit cells separated by LaO layers. Hence, comparison with SrTiO_3 suggests that features A and B represent the oxygen-derived $2p$ states with an admixture of transition metal d states, i.e., $\text{Cu } 3d$ states in our case. This conclusion will be corroborated by a comparison with the calculations of Mattheiss in the context of Fig. 2 (to be discussed below). Feature C is due to carbon $2s$ emission and reflects a bulk contamination. The D structure represents the $\text{La } 5p_{3/2}$ emission.¹⁴

The photo cross section at $h\nu=40.8$ eV gives about equal spectral weight to s , p , d , and f electrons¹⁵ so that the occupied electronic structure is quite well represented by the UPS curve in Fig. 1. On first sight, this seems to be different for the unoccupied states measured by inverse photoemission, since a photon energy of $h\nu=9.5$ eV has too low a cross section for f electrons.¹⁵ However, it was pointed out by Osterwalder and co-workers¹⁶ that $4f$ emission is indeed observable at an isochromat energy of 9.5 eV for lanthanum and some of its compounds, if there is enough hybridization between the spatially quite extended $4f$ wave function and unoccupied s and p states. In particular, a double-peak structure was reported¹⁶ for oxidized La at 4.4 and 6.6 eV above E_F and associated with the $4f$ emission of La_2O_3 . In analogy, we interpret the spectral features E at 7.2 eV and F at 9.5 eV in Fig. 1 as $\text{La } 4f$ emission, which is riding on a rather structureless unoccupied DOS consisting of $\text{Cu } s, p$ states, $\text{La } 5d$ and $\text{Sr } 5s$ states, closely resembling the unoccupied DOS of

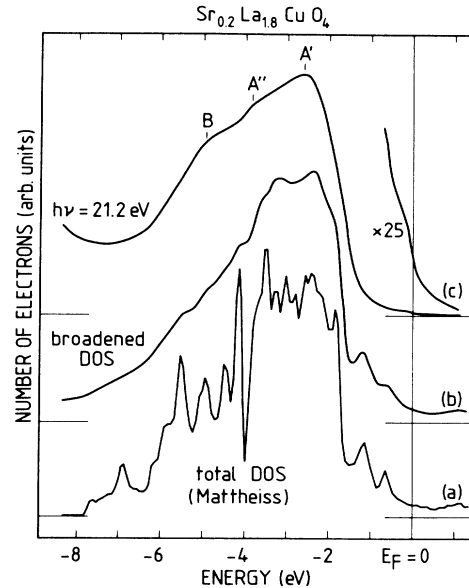


FIG. 2. (a) Total density of states (DOS) calculated for tetragonal La_2CuO_4 by Mattheiss (Ref. 9) using the LAPW method. (b) Calculated DOS convoluted with a Gaussian with $\text{FWHM}=0.2$ eV and a Lorentzian with an energy-dependent FWHM to simulate the lifetime broadening (see text). (c) Ultraviolet photoemission spectrum of $\text{Sr}_{0.2}\text{La}_{1.8}\text{CuO}_4$ at $h\nu=21.2$ eV; features A' , A'' , and B are discussed in the text.

SrTiO_3 (Ref. 13). All the latter states are possibly hybridizing with the empty $4f$'s, and this would allow them to be observed at this rather low photon energy.¹⁶ Such an interpretation is consistent with the calculated band structure⁹ where antibonding bands formed by $\text{Cu } d(x^2-y^2)$ and $\text{O } p(x, y)$ states cross the Fermi level and merge into the flat $4f$ bands above 4 eV. The strong dispersion of these Cu-O bands accounts for the low spectral intensity right below and above E_F in Fig. 1, while a higher DOS associated with flat bands at 1.1, 1.8, and 1.9 eV at the Z , Γ , and X symmetry points, respectively, are responsible for the increasing intensity forming a conduction-band type of emission feature above 2 eV in Fig. 1.

In Fig. 2 we have plotted as curve (a) the total DOS for tetragonal La_2CuO_4 as calculated by Mattheiss⁹ using a self-consistent version of the linear-augmented-plane-wave (LAPW) method.¹⁰ Also shown is a 21.2 eV photoemission spectrum which we want to compare with the spectrum of Fig. 1 taken at $h\nu=40.8$ eV. The photo cross-section ratio $\text{O } 2p/\text{Cu } 3d$ decreases from 1.7 to 1.1 in going from 21.2 to 40.8-eV photon energies.¹⁵ This lets us conclude that the more enhanced Fermi-level emission at $h\nu=40.2$ eV, in Fig. 1 as compared to Fig. 2 ($\times 10$ vs $\times 25$ insets), contains the higher angular-momentum character. As mentioned above, this is consistent with the Cu-O antibonding states crossing E_F in the Mattheiss calculation.⁹ Furthermore, feature A' and A'' at -2.6 and -3.8 eV, respectively, merge into a stronger peak A at -3.3 eV in Fig. 1, where the more-or-less pure $\text{Cu } 3d$

bands are located.⁹ At lower energies (-4 to -6 eV) oxygen-derived $2p$, as well as the bonding Cu-O bands, form a broad feature associated with the structure B in Figs. 1 and 2. Its intensity relative to the minimum at -7.5 eV is decreasing when going to higher photon energies indicating its lower angular-momentum character.

Next we discuss the direct comparison of experiment and theory in Fig. 2 in more detail. As curve (a) we have plotted the total DOS of La_2CuO_4 calculated⁹ by the LAPW method. To simulate our experimental energy resolution of 0.2 eV we have convoluted this curve with a Gaussian with a full width at half maximum (FWHM) of 0.2 eV. In addition, convolution with a Lorentzian which has an energy-dependent FWHM $\Gamma(\text{eV}) = 0.05(E - E_F)^2$ accounts for a weak lifetime broadening.¹⁷ The resulting broadened DOS is plotted as curve (b) in Fig. 2. Although photoemission cross-section effects discussed above are completely neglected, the agreement of this theoretical curve with the measured UPS curve (c) for $\text{Sr}_{0.2}\text{La}_{1.8}\text{CuO}_4$ is quite good with respect to gross peak positions and overall shape. How the various peaks A' , A'' , and B may be associated with the Cu $3d$ and O $2p$ band states has been discussed above. Fine structure in the broadened DOS (b), which is not accounted for in the measured spectrum (c), is attributed to the DOS of pure La_2CuO_4 , which may be smeared out by the random substitution of La by Sr in the present $\text{Sr}_{0.2}\text{La}_{1.8}\text{CuO}_4$ sample.

An interesting point is the position of E_F relative to the top of the valence band. We have used the midpoint of the theoretical VB edge to align the calculated DOS for tetragonal La_2CuO_4 with the UPS curve for $\text{Sr}_{0.2}\text{La}_{1.8}\text{CuO}_4$. This shifts the calculated⁹ Fermi level

from 1.07 to 1.6 eV above the VB edge, although substitutional alloying of trivalent La with divalent Sr should lower its energetic position. It is suggested⁹ that a gap straddling E_F exists in pure La_2CuO_4 because of the Peierls distortion or breathing-type displacements of the O atom away from the Cu site. This would go along with the original suggestion¹ that Jahn-Teller-type polarons exist in these oxides. The alloy-induced Fermi-level shift would eliminate these distortions and provide states at E_F with a strong coupling to the oxygen vibrations,⁹⁻¹¹ thus enhancing T_c . A future photoemission study of $\text{Sr}_x\text{La}_{2-x}\text{CuO}_4$ as a function of stoichiometry x will clarify the role of the Fermi level.

In summary, we have provided first measurements of the electronic structure of the high- T_c superconductor $\text{Sr}_{0.2}\text{La}_{1.8}\text{CuO}_4$ and compared it with LAPW band-structure calculations for tetragonal La_2CuO_4 . Although the overall agreement is quite good, there are questions with regard to the Fermi-level position relative to the valence-band edge as a function of the substitutional alloying of La with Sr.

Note added in proof. During the preparation of this manuscript, another band-structure calculation was published¹⁸ together with Ref. 9 which was made available to us before publication. The electronic structure of both calculations are quite similar and both point out the essential role of the Cu $3d$ -O $2p$ interaction and the Fermi-surface instability.

We are grateful to H. Schmid, M. Tschudy, and D. Widmer for their expert assistance with the sample preparation and measurements.

¹J. G. Bednorz and K. A. Müller, *Z. Phys. B* **64**, 189 (1986).

²J. G. Bednorz, M. Takashige, and K. A. Müller, *Europhys. Lett.* **3**, 379 (1987).

³S. Uchida, H. Takagi, H. Kitazawa, and S. Tanaka, *Jpn. J. Appl. Phys.* **26**, L1 (1987).

⁴C. W. Chu, P. H. Hor, R. L. Meng, L. Gao, Z. J. Huang, and Y. Q. Wang, *Phys. Rev. Lett.* **58**, 405 (1987).

⁵R. J. Cava, R. B. van Dover, B. Batlogg, and E. A. Rietman, *Phys. Rev. Lett.* **58**, 408 (1987).

⁶M. K. Wu, J. R. Ashburn, C. J. Torng, P. H. Hor, R. L. Meng, L. Gao, Z. J. Huang, Y. Q. Wang, and C. W. Chu, *Phys. Rev. Lett.* **58**, 908 (1987).

⁷P. H. Hor, L. Gao, R. L. Meng, Z. J. Huang, Y. Q. Wang, K. Foster, J. Vassilios, C. W. Chu, M. K. Wu, J. R. Ashburn, and C. J. Torng, *Phys. Rev. Lett.* **58**, 911 (1987).

⁸J. G. Bednorz, M. Takashige, and K. A. Müller, *Mater. Res. Bull.* (to be published); and (unpublished).

⁹L. F. Mattheiss, *Phys. Rev. Lett.* **58**, 1028 (1987).

¹⁰L. F. Mattheiss and D. R. Hamann, *Phys. Rev. B* **28**, 4227 (1983).

¹¹W. Weber, *Phys. Rev. Lett.* **58**, 1371 (1987).

¹²B. Reihl, *Surf. Sci.* **162**, 1 (1985).

¹³B. Reihl, J. G. Bednorz, K. A. Müller, Y. Jugnet, G. Landgren, and J. F. Morar, *Phys. Rev. B* **30**, 803 (1984).

¹⁴*Photoemission in Solids*, edited by M. Cardona and L. Ley (Springer-Verlag, New York, 1978).

¹⁵S. M. Goldberg, C. S. Fadley, and S. Kono, *J. Electron. Spectrosc. Relat. Phenom.* **21**, 285 (1981).

¹⁶J. Osterwalder, *Z. Phys. B* **61**, 113 (1985); J. Osterwalder, T. Riesterer, and L. Schlapbach, *J. Less-Common Met.* **111**, 295 (1985).

¹⁷J. B. Pendry and J. F. L. Hopkinson, *J. Phys. F* **8**, 1009 (1978).

¹⁸J. Yu, A. J. Freeman, and J. H. Xu, *Phys. Rev. Lett.* **58**, 1035 (1987).